Colloid Polym Sci 274:772–778 (1996)
© Steinkopff Verlag 1996

ORIGINAL CONTRIBUTION

J. Santhanalakshmi
K. Anandhi

Formations of polyvinyltoluene microlatexes in quaternary oil in water cetyltrimethylammonium bromide microemulsions

Received: 7 October 1995
Accepted: 10 January 1996

Dr. J. Santhanalakshmi (✉) · K. Anandhi
Department of Physical Chemistry
University of Madras
A.C. College Campus, Guindy
Madras 600 025, Tamil Nadu, India

Abstract Polymerization of vinyltoluene (VT) in quaternary microemulsions containing cetyltrimethylammonium bromide (CTAB) as the cationic surfactant is studied using laser Raman spectroscopy (LRS) and dilatometry. The influences of water soluble (potassium peroxodisulphate, ammonium peroxodisulphate) and oil soluble (azobisisobutyronitrile, benzoyl peroxide) initiators, monomer, surfactant, cosurfactants (*n*-alcohol and bifunctional alcohols) and temperature on the rates of polymerization (R_p), energy of activation (Ea), particle diameter (D), number of polymer particles (N_p), molecular weight of polyvinyltoluene ($\bar{M}_v$) and number of polymer chains per latex particle (N_{pc}) are investigated. The dependencies of the kinetic and latex size parameters on the initiators and cosurfactants are discussed in terms of the efficiency of the initiators in initiating the polymerization and on the interfacial partitioning behavior of various cosurfactants. The polymerization mechanism seems to follow Smith Ewart Case II hypothesis with two distinct rate regions. Final polymer microlatexes are found to lie within 10–50 nm as observed by transmission electron microscopy (TEM). Molecular weights are in the range of (1 to 5) $\times 10^6$. Each latex particle contains one to three polymer chains.

Key words Vinyltoluene polymerization – microemulsion polymerization – dilatometry – laser Raman spectroscopy – polymer microlatexes – transmission electron microscopy – interfacial partitioning

Introduction

Production of stable monodisperse microemulsion (μE) suspensions of homopolymer microlatexes is a subject of current interest [1–2]. Size, stability and utility of the microlatexes may be controlled through the microstructure of μE droplets [1–3]. Among vinyl monomers, styrene and methylmethacrylate o/w μEs polymerizations are extensively investigated. A few reports on alkyl ring substituted styrene like vinyltoluene (VT) exist only for emulsion polymerization systems [13]. Methyl substitution ($+I$ effect) renders greater resonance stability of the propagating radicals which lowers the rate of polymerization (R_p) in the emulsion medium [13]. Since μEs serve as a media for enhanced rates [14] VT – μE polymerization would be an interesting case study.

Recently, VT-sodium dodecylsulphate (SDS) o/w μE polymerization with enhanced R_p compared to emulsion and bulk with nearly monodisperse latexes of high molecular weight ($\bar{M}_v$) have been verified [15–17]. When SDS is replaced by cetyltrimethylammonium bromide (CTAB), the positively charged droplet interfaces may be expected to alter R_p, monomer and cosurfactant (CS) interfacial

partitioning, and the stability of the μEs. If initiators (I) like potassiumperoxodisulphate (KPS) and ammoniumperoxodisulphate (APS) are used, the presence of positively charged micelle interfaces may create an attraction on the SO_4^- produced by the decomposition of the initiators in the water phase and thereby alter R_p values. In the present study, investigations on VT-CTAB μE polymerization and influences of I, CS, CTAB, VT and temperature on kinetic parameters, particle size and $\bar{M}_v$ of the polymer are studied. Laser Raman spectroscopy (LRS) and dilatometry are utilized to monitor the kinetics of polymerization. Transmission electron microscopy (TEM) and viscosity average molecular weights ($\bar{M}_v$) are used to characterize the final microlatexes.

Experimental section

VT from Fluka was vacuum distilled under reduced pressure. CTAB from Sd.Fine, India was recrystallized from methanol mixture. *n*-Propanol (PrOH), *n*-butanol (BuOH), *n*-pentanol (PeOH), butylcarbitol (BuCa), carbitol (Ca), ethylcellosolve (ECe) and butylcellosolve (BuCe) from Sd.Fine, India, were distilled under reduced pressure. Recrystallized samples of azobisisobutyro nitrile (AIBN) and benzoyl peroxide (BP) (Kodak Chemicals, India) and APS and KPS (Aldrich) were used. Triple distilled water was used for all experiments. The o/w μEs region (L_1) at 30 °C was determined by titrating the mixture of VT, water and CTAB with CS until transparency. All μEs were sealed, thermostated and N_2 purged for about 40 min for replacement of air/O_2 before their use in dilatometry and LRS. At 70 °C, hydroquinone was added to VT to inhibit thermal polymerization.

The LRS spectra were obtained with a Cary Model 82 laser Raman spectrometer with a Coherent Innova-70 Argon Laser (4880 Å) as the source following an earlier reported procedure [16]. Polymerization by dilatometry was carried out in a 20 ml capacity double-walled dilatometer assembly through which thermostated water was circulated and fitted with a 40-cm-long capillary (i.d. 1 mm). Caliberation of the capillary height with conversion curves was made by gravimetric method. The slopes of the percentage conversion-time plots were used for R_p determinations.

One drop of polymerized latex was added to 2 ml of 2% phosphotungstic acid solution and one drop of this mixture was put on a Formvar-coated copper grid of 400 mesh and photos were taken using a Philips 400 Transmission Electron Microscope. The particle diameter (D) was measured by the Zeiss MOP-3 Analyser. The polymerized μE latexes were precipitated in excess of methanol and washed with excess methanol to remove CTAB and dried in vacuum at 45 °C. $\bar{M}_v$ of the polymer was determined at 30 °C by Ubbelohde dilution viscometer.

Results and discussion

Monophasic μEs from water corner and extending towards oil corner at 30 °C is similar but slightly greater than at 70 °C (Fig. 1A). This is due to the temperature-dependent μE droplet breakdown leading to phase separations. Beyond the phase boundaries, bicontinuous and oil-rich regions ensue. Due to the hydrophilic nature of BuCa and interfacial partitioning of VT, the monophasic regions are found to be larger in area for these systems as compared to other CSs (Fig. 1B). For a fixed ratio of BuCa/CTAB (1.12), maximum solubilization of VT upto 12% is obtained. Increase in CTAB increases the μE region near water corner (Fig. 1C). At fixed weight proportions of VT, BuCa and water, an increase in CTAB/VT ratio above 0.8 results in the single phase μEs becoming more translucent.

Fig. 1 Partial pseudoternary phase diagrams (wt %) of vinyltoluene (VT)-CTAB (C)-water (W)-alcohol microemulsions. ○ = VT + alcohol; ⋆ denote compositions utilized for polymerization. **A** O = VT + BuCa; (—) 30 °C; (××) 70 °C **B** At 30 °C O = VT + BuCa (—); VT + BuCe (···); VT + PeOH (—·—) **C** At 30 °C; O = VT + BuCa; C = 0.274 M (—); 0.206 M (···); 0.137 M (– – –)

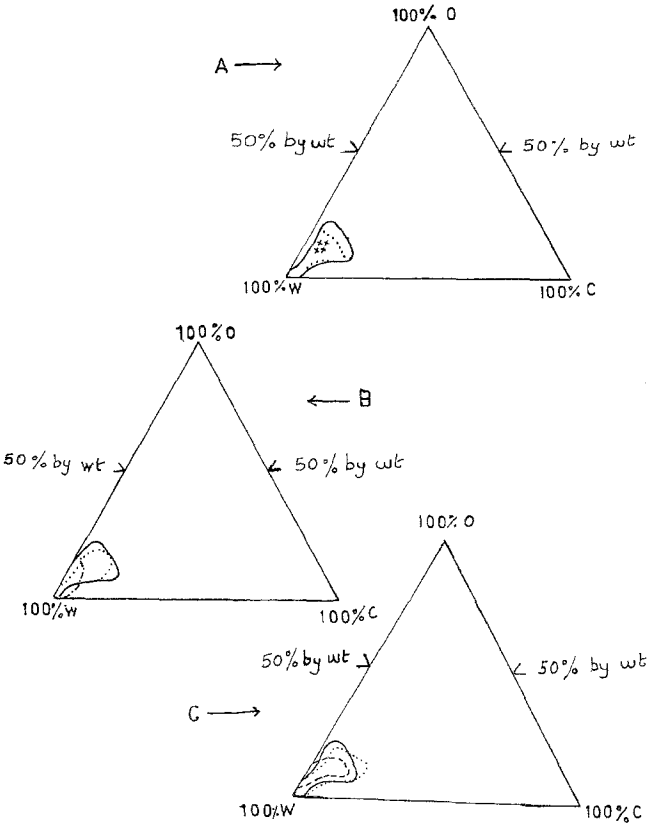

Colloid & Polymer Science, Vol. 274, No. 8 (1996)
© Steinkopff Verlag 1996

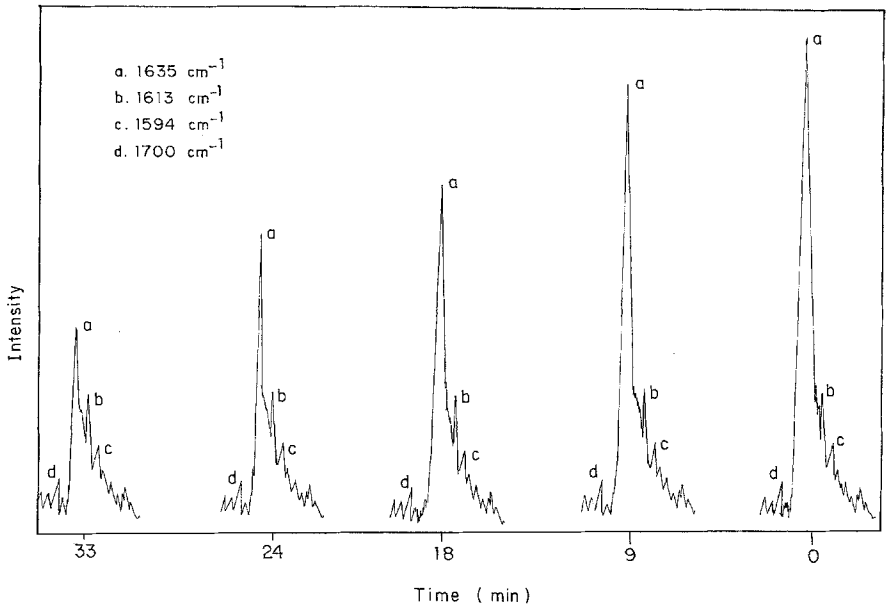

Fig. 2 A typical LRS variation of C=C peak intensity with time for vinyltoluene-CTAB microemulsions at 70 °C. [KPS] = 1.0 mM; [CTAB] = 0.207 M; [VT] = 0.57 M

When this ratio exceeds 1.5, a highly viscous, bluish and flaky surfactant-rich phase is obtained.

The LRS intensity variation of C=C peak (1635 cm^{-1}) of the monomer with time was used to evaluate R_p. A linear relationship between the monomer concentration and integral area of the peak was observed in agreement with earlier reports [8, 16]. The base peaks B, C and D (Fig. 2) do not pertain to vinyl group. The dilatometric and LRS measurements concur with each other. The values of the rate of polymerization obtained for 5% conversions are considered as R_{pi} values.

Two stages of polymerization rates occur in the present system (Fig. 3). In Step I, the rate increases due to the increase in the number of the nucleation loci and reaches a maximum (R_{pmax}) when all the noninitiated monomer swollen droplets have disappeared by diffusion of the monomer to the growing particles. In Step II, due to the consumption of the monomer within the growing polymer particles, the rate decreases (Fig. 3). Such two-stage intervals have been reported earlier in μEs [4, 7]. For APS and KPS systems the kinetic values are identical. Hence KPS system is considered for discussion. R_{pmax} is achieved at 15–20% for AIBN and BP while for KPS and APS at 20–25% conversions.

Longer I_p values and slightly lower rate values are obtained in CTAB-VT μEs compared to the SDS-VT μEs reported earlier [16]. This may be due to the attraction of the $SO_4^{\cdot-}$ radicals on the CTAB droplet interfaces, which lengthens the residence time of the primary radicals on the droplet interface. This increases I_p (Fig. 6) and decreases R_{pi} (Fig. 4). R_{pi}, $\bar{M}_v$ and number of polymer particles (N_p) dependency powers of KPS, AIBN, BP vary slightly while R_{pmax} dependencies are invariant (Table 1).

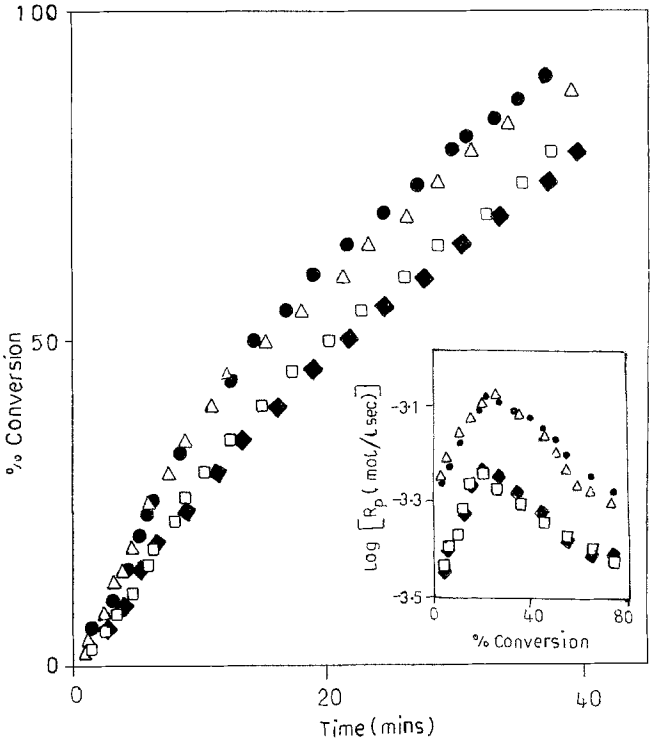

Fig. 3 Percentage conversion versus time plots for 1.0 mM initiator concentrations at 70 °C. [VT] = 0.57 M; [CTAB] = 0.206 M. (Δ) KPS; (●) APS; (♦) AIBN; (□) BP. Inset: Log R_P versus conversion for the system of composition as in Fig. 3. (△) KPS; (●) APS; (♦) AIBN; (□) BP

Based on the decomposition rate constants (k_d) of the I [18a] the radical generation rates of 1.0 mM KPS, AIBN and BP are 4.66×10^{-8}, 7.6×10^{-8} and 3.66×10^{-8} mol/L.s respectively, indicating that concentration of

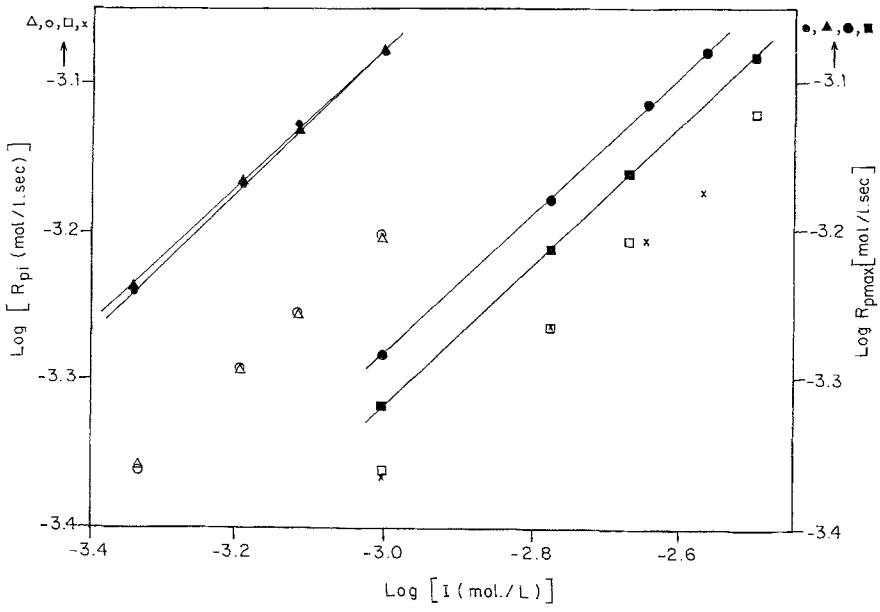

Fig. 4 Variation of $\log R_{pi}$ and $\log R_{pmax}$ (filled symbols) with initiator concentrations. (○, ●) KPS; (△, ▲) APS, (□, ■) AIBN; (×, ●) BP

primary radicals fall in the order AIBN > KPS > BP. Hence, in case of BP, lower values of R_{pi} (Fig. 4) and higher I_p values than KPS (Fig. 6) and AIBN (Fig. 7) are seen. In case of AIBN, decomposition produces uncharged cyanoisopropyl radicals which can diffuse out of the droplet to the aqueous phase. This lowers the AIBN efficiency (R_{pi} low) (Fig. 4). For the AIBN and BP systems the initiation in the droplets is limited by droplet volume, viscosity increase (cage effect), desorption and subsequent terminations of the radicals. These processes reduce the efficiency of the radicals. The reentry of the desorbed radicals may also contribute to droplet nucleations. Similar effects of desorption and reentry on emulsion polymerization has been well described by Nomura's theory [19]. For all initiators R_{pi} values increase with I since droplet initiations and number of nucleated droplets in μE increase proportionately with I. The propagating loci attains a maximum rate depending upon the droplet monomer composition and remains invariant towards I type. Hence a constant dependency of R_{pmax} on $[I]$ for all initiators is observed (Table 1).

$\bar{M}_v$ values exhibit a decreasing trend with increasing $[I]$, due to the increasing number of chain terminations. From the TEM photos of the polymer microlatexes (Fig. 5), the mean volume diameter (D) and N_p values are noted. N_p values increases with $[I]$, since the number density of the nucleated droplets increase with $[I]$ (Figs. 6 and 7). Decrease in D values with $[I]$ is due to the lesser availability of propagating monomers as well as increase in radical termination steps. Hydrophobic initiators (AIBN, BP) seem to produce particles with higher D values (Fig. 7) than hydrophilic KPS and APS systems (Fig. 6).

Table 1 Kinetic parameters of vinyltoluene-water-CTAB-butylcarbitol o/w microemulsion polymerizations

Initiator	R_{pi}^a	R_{pmax}^a	VT[b]	N_p^a	R_{pi}^c	I_p^c
KPS	0.48	0.48	1.20	0.37	0.05	0.22
APS	0.46	0.47	1.16	0.37	0.05	0.23
AIBN	0.48	0.49	1.04	0.37	0.01	0.06
BP	0.46	0.49	1.09	0.38	0.01	0.07

The values given in the table are slopes of log–log plots.
[a] $\log R_{pi}$, $\log R_{pmax}$ and $\log N_p$ versus $\log[I]$.
[b] $\log R_{pmax}$ versus log[VT] in presence of various initiators.
[c] $\log R_{pi}$ and $\log I_p$ versus log[CTAB].

N_p depends on the number density of the nucleated droplets and on $[I]$ (Figs. 6 and 7). High values of $\bar{M}_v$ and low values of N_{pc} (2–3 polymer chains per droplet) indicate that contribution to mechanism of chain deactivation is mainly from the interfacial chain transfer of the free radicals which is one of the mode of desorption of radicals. With increase in $[I]$ the % yield increases. The dependency of R_{pmax} and N_p on $[I]$ is quite consistent with the prediction of 0.48 and 0.4 by Smith Ewart Case II hypothesis and hence the same mechanism may be envisaged here. R_{pmax} and D values at lower [KPS] equal those at higher [AIBN] and [BP]. In KPS systems initiator radicals are available to all droplets for initiation. Thus a single KPS radical is equivalent to 1–3 radicals of BP and 3–5 radicals of AIBN in nucleating a droplet. This makes KPS/APS more efficient than AIBN and BP (Table 2).

Toluene and dodecane are used as dilutents to study monomer effect. For all I, R_{pi} and $\bar{M}_v$ increases wtih [VT]

Colloid & Polymer Science, Vol. 274, No. 8 (1996)
© Steinkopff Verlag 1996

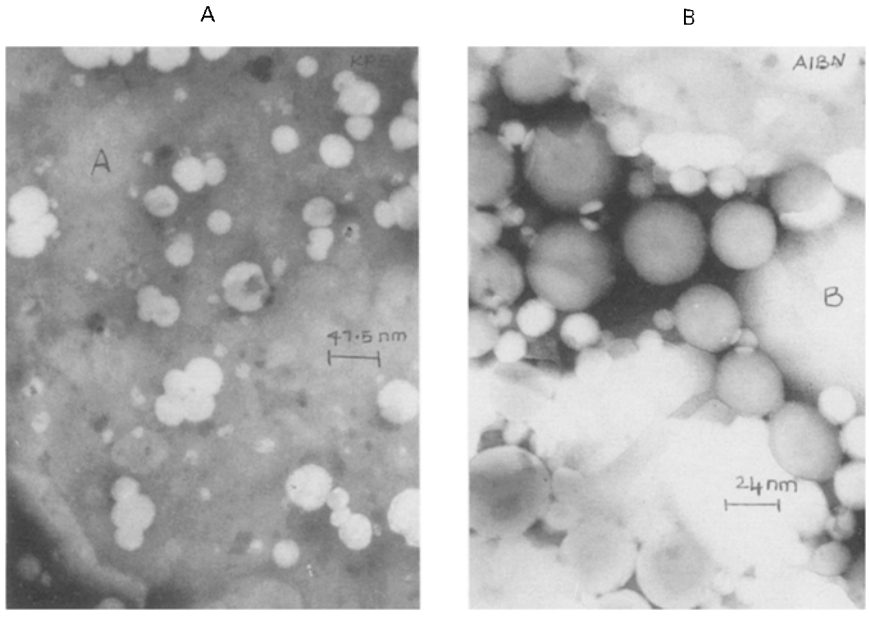

Fig. 5 TEM photographs of polyvinyltoluene microlatex obtained from vinyltoluene - CTAB-BuCa- water micro-emulsion polymerization initiated by **A** KPS and **B** AIBN

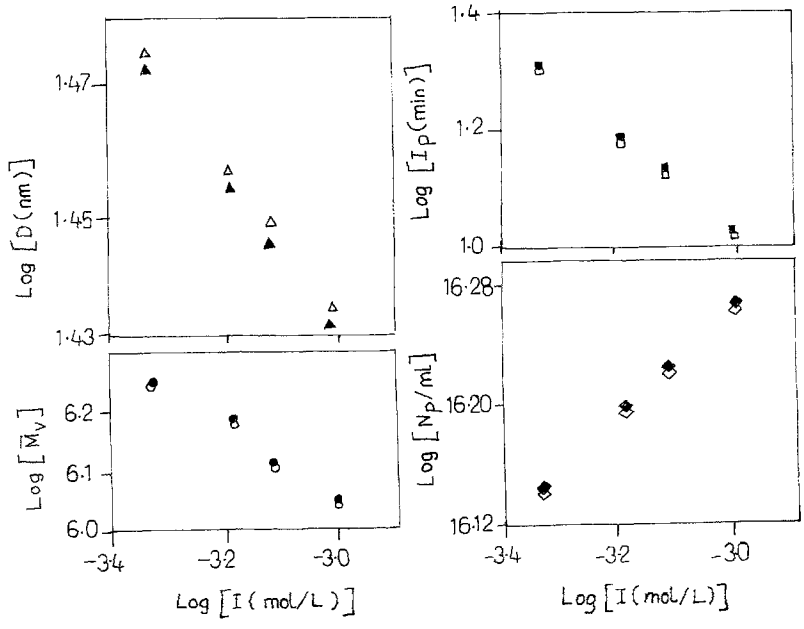

Fig. 6 Variation of log I_p, log $\bar{M}_V$, log D and log N_p with KPS (filled symbols) and APS (open symbols) concentrations

at constant CTAB due to increased availability of the monomer within each droplet. Due to increase in chain transfers to the solvent, rate dependencies greater than 1 are obtained. Since [CTAB] is greater than CMC the number density of the oil swollen droplets is greater than the number of free radicals generated and the number density of the droplets which deplete during polymerization. Hence R_p and $\bar{M}_v$ values remain unaltered. However the I_p values of persulphate initiators show a greater dependency on [CTAB] than AIBN and BP due to the positive interface and SO_4^- radicals interaction (Table 1). Increase in [CTAB], increases the number density of the droplets consequently decreasing the particle size (Fig. 8).

For all I, the cosurfactant (CS) effect on the dependency parameters remains the same (Table 3). Variations are observed due to differences in chain transfers to the CSs. Unlike bifunctional CSs, R_{pi} remains invariant in monofunctional CSs. Due to enhanced solubilization of

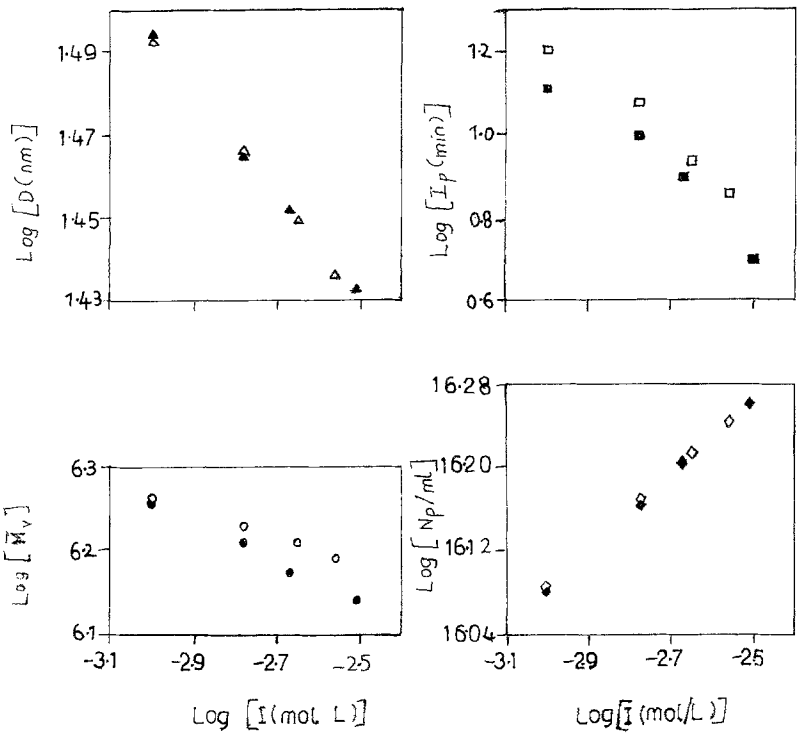

Fig. 7 Variation of $\log I_p$, $\log \bar{M}_v$, $\log D$ and $\log N_p$ with AIBN (filled symbols) and BP (open symbols) concentrations

Table 2 Similar polymer microlatex features of o/w vinyltoluene microemulsion polymerizations. System considered water (82.4%); vinyltoluene (5.5%); butylcarbitol (5.9%); CTAB (6.2%)

Features	Initiator Types KPS	AIBN	BP
Concn. (mM/L)	1.00	3.13	2.67
R_{pmax} (10^{-4}mol/L.sec)	8.33	8.29	8.34
D (nm)	27.0	27.1	27.3
N_p (10^{15}/ml)	18.6	18.4	17.6
Rate of free radical generation (10^{-8}mol/L.sec)	4.66	23.7	9.77
1 KPS radical equivalent to	–	5.0	2.1

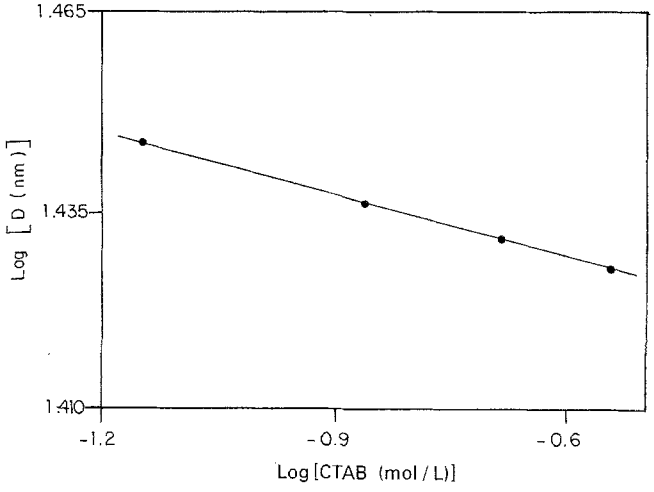

Fig. 8 Variation of particle diameter (D) (●) with CTAB concentrations [KPS] = 1.0 mM; [VT] = 0.5 M

VT by bifunctional CSs, larger latexes are obtained with bifunctional CSs. From the known chain transfer constants of a few alcohols [18b], it can be observed that chain transfer is not much affected by CS type. Hence the variation in $\bar{M}_v$ in presence of various CSs can be effectively attributed to difference in CS interfacial partitionings and the influences on the termination processes. The overall activation energy (Ea) is found as 12–22 Kcals/mol. Unlike SDS-μEs [16] wherein Ea is independent of type of initiator. Ea is slightly higher for KPS/APS-CTAB μEs (21.6 Kcals/mol) than AIBN (13.5 Kcals/mol) and BP μEs (13.0 Kcals/mol). Since the decomposition energies of the initiators are comparable [18] the Ea difference is due to the increased energy barrier caused by the positive droplet interface over $SO_4^{\cdot-}$ radicals. Ea is dependent on the CS type due to the increase in the interfacial partitioning, fluidity and curvature of the interfaces that consequently alters the potential barrier for initiation and other subsequent steps. R_{pmax} values are found to be 3–4 times greater than styrene counterpart [7]. In VT, the methyl group of the aromatic ring seems to cause greater stabilization of the propagating radicals through the

© Steinkopff Verlag 1996

Table 3 Kinetic parameters of vinyltoluene-CTAB, o/w microemulsion polymerization with different cosurfactants [VT] = 0.57 M; [KPS] = 0.47 mM; [CTAB] = 0.207 M

CS	[KPS][a]	[VT][b]	Ea Kcals/mol	$\bar{M}_V \times 10^6$	D nm
BuCa	0.48	1.20	21.6	1.79	29.7
Ca	0.44	1.17	20.98	1.70	28.8
BCe	0.48	1.2	20.2	1.53	28.3
Ce	0.45	1.18	19.23	1.40	27.3
PeOH	0.41	1.10	18.28	1.51	26.0
BuOH	0.39	1.22	15.38	1.24	25.1
PrOH	0.39	1.24	13.54	1.09	23.7

[a] The values are slopes of $\log R_{pmax}$ versus log[KPS] plots.
[b] The values are slopes of $\log R_{pmax}$ versus log[VT] plots.

hyperconjugation effect. The methyl group of the aromatic ring seems to cause greater stabilization of free radicals and more residence time of radicals.

Conclusions

In VT polymerization aided by CTAB, KPS is found to be a more efficient I than AIBN and BP. BuCa, as the CS seems to produce higher dependencies of kinetic parameters with $[I]$. Lower Ea values are seen for propanol-containing microemulsions. On comparing SDS-VT μEs, I_p and Ea values are increased in the presence of hydrophilic initiators. This is due to the electrostatic interaction of positive CTAB droplet interface with $SO_4^{\bar{}}$ radicals. Higher R_{pmax} values seen for VT μE polymerization than for styrene μE polymerization is due to the methyl substitution in the aromatic ring.

Acknowledgment The authors thank UGC-India, for their financial help. They also acknowledge CDRI, Lucknow-India for the TEM results.

References

1. Antoniettii M, Bremser W, Muschenborn D, Rosenaur C, Schupp B, Schmidt M (1991) Macromolecules 24:6636
2. Antonietti M, Lohmann S, Van Neil C (1992) Macromolecules 25:1139
3. Chi W (1994) Macromolecules 27:298
4. Guo JS, El-Aasser MS, Vanderhoff JW (1989) J Polym Sci Chem 27:691
5. Guo JS, Sudol ED, Vanderhoff JW, El-Aasser MS (1992) J Polym Chem 30:691 and 703
6. Gan LM, Chew CH, Lye I, Ma L, Li G (1993) Polymer 34:3860
7. Gan LM, Chew CH, Lye I (1992) Makromol Chem 193:1249
8. Feng L, Simon Ng KY (1990) Macromolecules 27:1053
9. Larpent C, Tadros TF (1991) Colloid Polym Sci 269:1171
10. Gan LM, Chew LM, Lian JH, Lee KC, Gan LH (1994) Colloid Polym Sci 272:1082
11. Gan LM, Lian N, Chew CH, Li GZ (1994) Langmuir 10:2197
12. Antonietti M, Rainer B, Lohmann S (1995) Makromol Chem Phys 196:441
13. Paoletti KP, Billmeyer Jr FW (1964) J Polym Sci Part A 2:2049
14. Fendler JH, Fendler EJ (1975) Catalysis in Micellar and Microemulsion Systems, Academic Press, New York
15. Santhanalakshmi J, Anandhi K (1995) J Surf Sci Technol 9, in press
16. Santhanalakshmi J, Anandhi K (1995) J Appl Polym Sci, in press
17. Santhanalakshmi J, Anandhi K (1995) Colloids Surf, in press
18. Brandrup J, Immergut EH (1975) Polymer Hand Book 3rd Edn, Wiley New York (a) Chap V; (b) Chap II
19. Nomura M (1982) In: Piirma I (ed) Emulsion Polymerization. Academic Press, New York, p 191